Critical Current Predictions Through Computational Intelligence for Main Commercial High-Temperature Superconducting tapes

Henrique Gomes Lourenço

henriquelourenco02@gmail.com
Instituto Superior Técnico, Lisboa

***Abstract*—Modeling High-Temperature Superconductive (HTS) tapes is a crucial step in the development of next-generation superconducting technology. In this work, mathematical models are extracted by applying machine learning algorithms and fitting empirical relations to a public database of experimental results on different manufacturers' HTS tapes, provided by the Robinson Research Institute.**

One method uses Gaussian Process Regression (GPR), where the models are trained and tested to predict DC critical currents given the operating conditions (temperature, applied magnetic field magnitude and angle). In order to produce accurate models, the data is preprocessed, hyperparameter optimization is applied and separate scale lengths are used for each predictor (Automatic Relevance Determination or ARD). Another method is to use two empirical models that are fitted to the data using only the magnetic field magnitude as the input: the Kim and Kim Plus models.

Comparing results, the GPR model provides the lowest relative errors, except for cases in which parallel external fields originate steep current curves. This method also requires high computation times to generate, unlike empirical modeling. The empirical models require a unique fit for each temperature/angle pair of the dataset. To address this, two new empirical models, named Custom and Advanced Custom models, which incorporate the field angle as an input, are proposed.

***Index Terms*—High-Temperature Superconductors (HTS); Critical Current; Machine Learning; Gaussian Process Regression (GPR); Empirical Modeling; Kim Model.**

I. Motivation

High-Temperature Superconductors (HTS) are a point of focus for current and future energy applications [1], with the potential to heavily decrease energy losses and increase the efficiency of the systems that support our society. The nearly zero resistance characteristic of HTS makes them a prime contender to be used in building new-generation electromagnets.

When there are multiple HTS coils conducting side by side the magnetic field created by the current flowing in one loop of each coil crosses all the other loops and contributes to lowering the critical current of the system, which separates superconductivity and normal conductivity. This intrusion also happens at many possible angles. The number of interactions is increased when these electromagnets are used in actual applications. This additional complexity, coupled with the fact that HTS materials are costly and manufacture procedures are involuted [2], demands a prior simulation analysis for optimal trajectory on any HTS engineering project.

There is a lack of publicly available information on the characterization of modern HTS tapes. With the purpose of changing this landscape, a team led by Dr. Nicholas M. Strickland and Dr. Stuart C. Wimbush, respectively principal scientist and research scientist at Robinson Research Institute [3], New Zealand, have, in 2014, designed "A 1 kA-class cryogen-free critical current characterization system for superconducting coated conductors" characterized in [4]. The results obtained from this testbench have been published on a public database, available in [5] and described in [6]. This database comprises a total of 20 datasets from 12 different companies, as to "increase understanding" on the critical current matter of HTS tapes and provide a "reference point for designers seeking to specify wire for the more efficient construction of high-temperature superconducting machines and devices" [6].

Essentially, having more data at the scientific community's disposal will increase the knowledge resolution, leading to a better description of the relationship between the critical current of an HTS tape and its operating conditions (such as temperature, applied magnetic field magnitude and its angle). In this work, Machine Learning (ML) algorithms and Empirical Modeling techniques are used to obtain mathematical objects that describe these relationships. In turn, these models can then be used in multiphysics simulation software [1] in order to predict the behavior of more complex designs.

Traditionally, in a simulation environment, the strategies used to estimate the critical current I_c in an HTS system, involve implementing a look-up table containing existing data, which is a limited endeavor. Because of the problems that are associated with this solution, this work starts with obtaining *blackbox* models through the Gaussian Process Regression (GPR) algorithm using the published database for 5 different kernels. Additionally, it also implements Automatic Relevance Determination (ARD) for potentially better results.

A traditional alternative to look-up tables is using an analytical equation [1], like the one formulated by Kim et al. in 1962 [7]. Some modern variations of this equation have emerged over the years [8]. These models are to be explored and tested using the described database, in order to verify their precision and usefulness. Finally, two customized models, named Custom and Advanced Custom models, are formulated to not only guarantee better performance but also solve problems that are associated with the initial models.

II. Machine Learning applied to the HTS Database

The chosen ML algorithm is the Gaussian Process Regression (GPR).

A. Model Development with Basic Kernels

Implementing a GPR can be done somewhat easily using MATLAB [9], which contains five built-in kernels that are widely popular and will be tested. The kernels to be studied are:

- Exponential
- Matern 3/2
- Matern 5/2
- Squared Exponential (RBF)
- Rational Quadratic (infinite sum of RBF)

The first step is to create the model by using the *fitrgp* [10] function inputting the temperature, the field, its angle and the corresponding critical current sheet density as the training data points which will yield the regression model. The kernel type is set to each one of the previously mentioned kernels which will produce five different models. Additionally, there are some concepts that have been enforced in order to maximize the probability of having an accurate/useful model:

- Only the data points that have temperatures that are multiples of 10 will be used to train the model (20 K$, 30$ K$, 40$ K...). This is to be able to analyze if the model has the potential to predict critical currents outside the range of values that were measured in the laboratory. Therefore, less than 50% of the entire dataset will be training data.
- The software is configured so that it, not only estimates but also automatically optimizes the hyperparameters of each kernel [10], including the noise parameter.
- The software is programmed to standardize the data prior to training the model in an attempt to decrease the errors. But why would this operation improve results? According to [11], most ML algorithms assume that the input data has mean zero, or $m(\boldsymbol{X}) = \mathbf{0}$, so standardizing the dataset will set its mean equal to zero. Additionally, standardizing data points leads to better hyperparameter estimation and less error when inverting the covariance matrix, which is an operation that is present in all GPR algorithms.
- Prediction method is set to "exact" - this guarantees that all training data is used and also allows access to the confidence intervals: a big advantage of GPR. The fit method has been set to "sd" - this means that a subset of the data is used to estimate the parameters of the model using the Quasi-Newton method, before optimizing the parameters. All else is left to default. [10]

B. Model Development with ARD Kernels

A potential way to achieve improvement of results is through the use of Automatic Relevance Determination (ARD) in order to configure the kernel function to use different length scale parameters for each of the predictors [12] [13]. Applying ARD will result in 2 additional hyperparameters to optimize (since there are 3 predictors), which increases the training time of the model. In conclusion, five more models are trained, composed of the ARD kernel variations of the models described in Section II-A.

Only the model with the highest performance will be showcased in this article.

III. Empirical Modeling applied to the HTS Database

A. Kim Model

In 1962, Kim et al. [7] introduced the analysis of the behavior of J_c as a function of the applied magnetic field and assumed that the local fields were the sum of applied fields and field created by currents induced in the material [8]. It was also assumed that J_c followed the power series expansion

$$\frac{a}{J_c} = H_0 + H + a_1 H^2 + a_2 H^3 + ... \tag{1}$$

where a and H_0 are supposed material constants that can be computed experimentally, H is the external magnetic field strength. This would imply that if the coefficients a_1, a_2, ... had a sufficiently small value, then this relation could be simplified and rewritten as

$$J_c(B) = \frac{J_{c0}}{1 + \frac{B}{B_0}} \tag{2}$$

where the parameter $a/H_0 = J_{c0}$ (the value of the critical current density when there is no magnetic field applied to the tape) and $H/H_0 = B/B_0$. By definition, J_{c0} value does not depend on the magnetic field nor its angle but changes with the HTS temperature.

The first empirical model to be analyzed in this article is the one in (2), the original Kim model [7]. It is important to highlight, that in this model, the critical current density is a function of only the absolute value of the applied magnetic field B. In the context of HTS tape simulations, this magnetic field is computed based on the material's macroscopic properties, such as resistivity, and circulating currents [1] but does not take into account phenomena such as Abrikosov vortex and the defects that hold it in place. When $B = 0$ T, then $J_c = J_{c0}$ (the starting point) and, as B increases, J_c decreases with an inverse proportion. The parameter B_0 describes the slope of the curve, i.e how fast the current will decrease (the lower B_0 is the faster the decrease). For this model, when $B = B_0$, then the current density drops to half. The speed of the critical current density decrease also depends on the other operating conditions like the temperature and angle of incidence of the magnetic field.

B. Kim Plus Model

More complex models are created to be analyzed [8]. The assumption in (1) is substituted by

$$\frac{a}{J_c} = H_0 + c_1 H + c_2 H^2 \tag{3}$$

where c_1 and c_2 are coefficients. Then, with some mathematical manipulation, this expression is extended as

$$J_c(B) = \frac{J_{c0}}{\left(1 + \frac{B}{B_0}\right)^{\beta}} \tag{4}$$

This second model, which is called Kim Plus for the purpose of this article, now allows to describe the shape of the current descent using the parameter β. This value has been described to be dependent on some microscopic characteristics of the HTS layer [1]. For $\beta = 0$, the critical current is modeled as constant (Bean's model, not studied in this thesis) and for $\beta = 1$, the previous model in (2) is obtained. Naturally, every value for $\beta > 0$ is mathematically possible and allowed. In order to distinguish this parameter and B_0, β characterizes the shape of the decrease and B_0 its speed.

C. Custom Kim Model

The objective is now to construct a model that incorporates the angle of the applied magnetic field as an input and is able to predict peaks caused by Stacking Fault and Ion Radiation-type defects (creating parallel and perpendicular critical current peaks, respectively). As a starting point, (5) can be used.

$$J_c(B, \phi_B) = \frac{J_{c0}}{\left(1 + \frac{B}{B_0} \cdot w_B(\phi_B)\right)^{\beta}} \tag{5}$$

This new factor w_B acts on the magnetic field B, transforming it into an effective field, B_{eff} [1].

The challenge is to find the equation that should best describe w_B. It is imperative that $w_B \geq 0$ as otherwise the denominator could be less than 1 and the model would compute values higher than J_{c0}, which is not possible. Additionally, it is useful for w_B to be smaller than 1, so that all its components are normalized and the general range of B_0 is not changed when compared to the previous models. The flux pinning caused by nanoparticle defects does not affect the angle dependence of the HTS material and is therefore incorporated into the rest of the model (i.e. does not enter the w_B expression). With all of this in consideration, w_B shall be decomposed into

$$w_B(\phi_B) = 1 - w_{SF}(\phi_B) - w_{IR}(\phi_B), \tag{6}$$

where w_{SF} and w_{IR} account for the normalized weights of the stacking faults and ion radiation-type defect components, respectively. One way of determining the shape of w_{SF} and w_{IR} is to start with estimating the value of B_0 and β of an experimental set of data (utilizing previous fits using (4)). Then, (5) is rearranged with respect to w_B and plotted (Figure 1). Because w_B is located on the denominator of (5), then here it is necessary to model the valleys in Figure 1. The decision made is that the parameters w_{SF} and w_{IR} need to be modeled with periodic impulses starting at approximately $90°$ and $0°$, respectively.

One possible way to achieve this is through a variation of the normal distribution. Consider e^x where $x \in [-\infty; 0]$. With this limitation on x then the output of the exponential will be between 0 and 1. A cosine is a function that will rotate its output between 1 and -1 periodically. Subtracting 1 to this cosine will naturally decrement the output and will alternate between 0 and -2. This expression can then be put in the exponent of the exponential (i.e. it will substitute x) and will result in a mathematical shape shown in Figure 2 (purple).

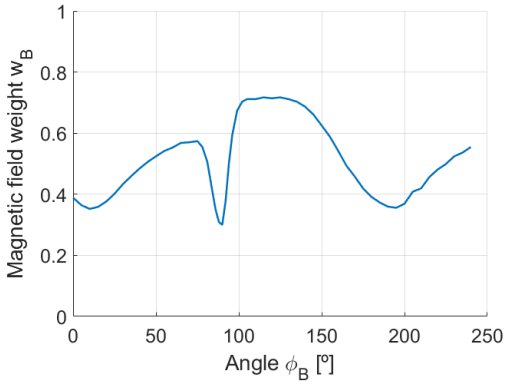

Figure 1: The weight applied to the B/B_0 fraction w_B plotted as a function of magnetic field angle using SuperPower dataset for 77.5 K; 2 T.

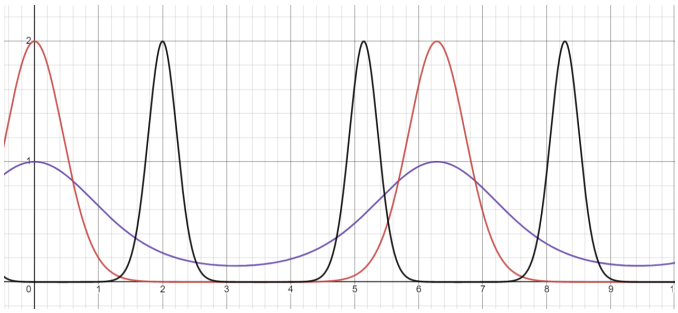

Figure 2: Example of periodic normal distribution-like functions. In purple: $e^{cos(x)-1}$. In red: $2e^{5(cos(x)-1)}$. In black: $2e^{5\left[cos\left(2\left(x-\frac{\pi}{2}\right)\right)-1\right]}$.

Notice how the peaks do not touch the x-axis. By modifying the coefficient to the exponential and of the decremented cosine (red) it is possible to change the amplitude and width of the impulse. Smaller widths also mean that the valleys start approaching the x-axis since the output of that expression becomes lower than -2. Additionally, it is needed to double the frequency of the cosine because the peaks of each SF/IR happen twice per rotation of the tape. This, coupled with a lateral movement of the pulses makes it able to describe the multiple peaks of each phenomena with only 3 parameters and good enough precision (black). These parameters exist for both types of peaks and therefore the following naming convention was adopted:

- IR and SF represents the perpendicular and parallel peaks, respectively;
- The a, p and w subscripts represent the normalized amplitude, location deviation and width parameters of said peak;

The components of w_B are written as

$$w_{SF}(\phi_B) = SF_a \cdot e^{\left[SF_w\left(\cos\left(2\left(\phi_B - \frac{\pi}{2} - SF_p\right)\right)-1\right)\right]} \tag{7}$$

and

$$w_{IR}(\phi_B) = IR_a \cdot e^{\left[IR_w \cdot (\cos(2(\phi_B - IR_p))-1)\right]} \tag{8}$$

Finally, the complete model when substituting (7) and (8) into (6), followed by incorporating the result into (5).

D. Advanced Custom Kim Model

For reasons that will be explained in Section V, the parameters IR_a, SF_w and SF_p need to be decomposed into expressions that include a magnetic field dependence. Essentially, it is hypothesized that:

- IR_a should be 0 when $B = 0$ T and rapidly increases to a fixed number;
- The width of this same peak also seems to decrease as magnetic field increases, which would mean that SF_w is supposed to increase.
- The parallel peak, on certain conditions, will start at around $70°$ and rapidly converge into a value of around $90°$. Therefore, SF_p should increase from around $-20°$ to $0°$;

After trial and error, the equations that best describe the relationship between these 3 parameters and the magnetic field are:

$$IR_a(B) = IR_{af} \cdot \tanh(IR_{as} \cdot B) \tag{9}$$

$$SF_w(B) = SF_{wi} + SF_{wf} \cdot \tanh(SF_{ws} \cdot B) \tag{10}$$

and

$$SF_p(B) = -SF_{pi} \cdot \exp(-SF_{ps} \cdot B) + SF_{pf} \tag{11}$$

Added to the nomenclature are the subscripts i, f and s, which are related to the words *initial*, *final* and, *speed*, respectively.

E. Empirical Modeling Fitting Procedure

The parameters of these empirical models are computed through a process called curve fitting multiple times. For instance, in the case of the SuperPower AP sample, there are a total of 16 temperatures containing data for magnetic field angle spans of $0°$ to $240°$ (55 angles in total for each temperature). Therefore, since Kim and Kim Plus models are only dependent on the magnetic field magnitude B, then, for this sample, either model is fitted for each combination of temperature and angle, for a total of 880 (=16×55) fits (this is what implies the use of look-up tables). In the case of both customized models, there is only a need to fit each model 16 times, since both of them have incorporated the magnetic field B and angle ϕ_B.

The data is interpolated in evenly spaced steps so that each point has the same weight in the fit. This is enough fitting optimization for the Kim and Kim Plus models, but for the customized models, higher weights are attributed to the angles where the peak of the critical currents are manifested (for both the parallel and perpendicular peaks).

All of the following models have been trained/fitted using only data for $B \leq 3$ T. Additionally, from this point forward, all critical current plots will be presented in its sheet density form I_c/w_{tape} [A/cm] since most tapes have different values of width - the measured critical current values are approximately linearly proportional to width. Results and analysis will be made for SuperPower's AP sample due to its recent publication and relevance. Lastly, relative errors below 10% are considered good enough for the current prediction/modeling purpose.

IV. Machine Learning Results and Analysis

A way to visualize the performance of each model is to compute the relative error for each point of the domain and then plot the areas where this error is lower than 10%.

A. ARD Matern32 Kernel

The ARD variant of the Matern32 kernel is potentially the best choice of kernel to be implemented (Figure 3), as the whole domain is almost perfectly modeled for perpendicular magnetic fields. Regarding parallel fields, for high absolute

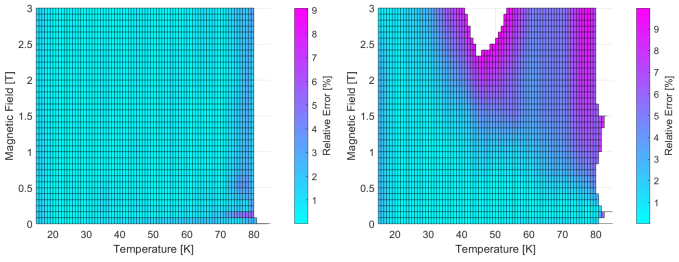

(a) $0°$ **(b)** $90°$

Figure 3: SuperPower AP critical current relative error ($\leq 10\%$) between database and GPR model with ARD Matern32 kernel predictions.

values (≥ 2 T) and intermediate temperatures (≈ 50 K), there are high errors, due to the fact that this is the region where this samples's parallel current peaks achieve their lowest widths. In fact, none of the models analyzed has the ability to keep up with these extremely high current slopes without heavily sacrificing precision in other areas of the domain.

B. Machine Learning Models Overview

Most of the computed models, have difficulty predicting the critical current of SuperPower AP sample at 77.5 K, especially for $90°$ angles. This could be potentially for two reasons: Firstly, this temperature is located towards the upper spectrum of available temperatures in this dataset, which means there is little data to train these models for both high and low temperatures. Another example of this happening is for the 15 K point, which is the lowest of the temperature spectrum and is also part of the test data (just like 77.5 K). Most models, especially the non-ARD variants tend to have high relative errors in both these data points. The second reason might have to do with the fact that critical current peaks in this at 77.5 K and ≥ 2 T tend to be very steep, just like at 45 K (the steepest). Indeed, even the best looking models have trouble modeling currents at the $90°$ angles for both temperatures, most likely because of the low amount of data points that describe these peaks. Further improvements are needed in order to adapt to them.

The definite issue with ARD implementation is that the computing times for this model was very high, more than 2 hours. Considering that the computing time of GPR increases cubically [14] with the number of entries makes it daunting to provide further inputs, or to apply it to other samples in the database.

V. Empirical Models Results and Analysis

A. Kim Model

Just like in Section IV, the relative error plots are made for analysis and are displayed in Figure 4. The Kim model

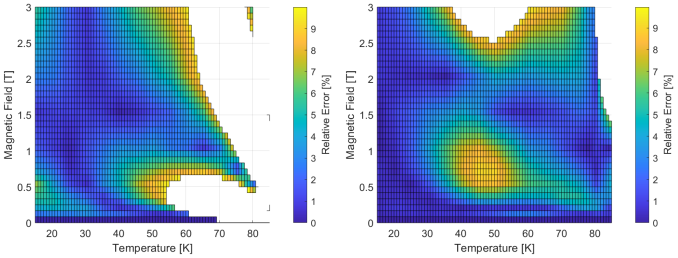

(a) 0° **(b)** 90°

Figure 4: SuperPower AP critical current relative error ($\leq$ 10%) between database and Kim model predictions.

is surprisingly good, and works well for large areas of the domain. However, for the worst case scenario (perpendicular field), and for high temperatures (most importantly 77.5 K), the relative error is always higher than the established limit. Therefore, the Kim model is not able to function the for most important operating conditions, that is, at the boiling temperature of nitrogen for the Superpower HTS sample.

Lastly, it is useful to look at the parameter B_0 to analyze how to behavior of the tapes change based on the operating conditions. As expected, and according to the meaning of

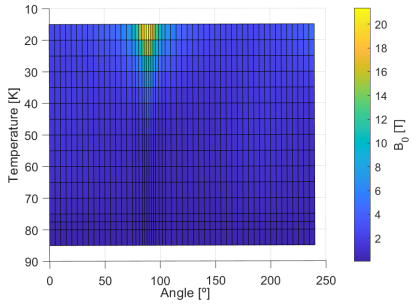

Figure 5: Parameter B_0 as a function of temperature and magnetic field angle for SuperPower AP.

B_0, as established in Section III, B_0 becomes smaller as the temperature increases, which means that the critical current will decrease faster with the same amount of magnetic field applied. For a perpendicular field, this parameter increases in an approximately linear fashion. Importantly, when decreasing the temperature, B_0 starts increasing abruptly at around the 45 K point and when the magnetic field is parallel to the tape. For these operating conditions, the samples are very robust to external magnetic field. In conclusion, the Kim model can be useful for an initial analysis of the behavior of HTS samples, but does not consistently model the critical current values for high temperatures.

B. Kim Plus Model

Figure 6 is equivalent to Figure 4, but using the Kim Plus model predictions instead. For the Superpower sample,

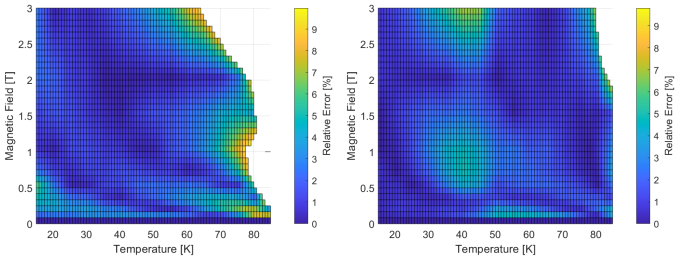

(a) 0° **(b)** 90°

Figure 6: SuperPower AP critical current relative error ($\leq$ 10%) between database and Kim Plus model predictions.

predictions are very accurate across the board. The only area where the model does not perform properly is when temperatures are higher than 80 K. Perhaps more importantly, for 77.5 K, the prediction are inaccurate for more than 2 T external perpendicular magnetic field. Additionally, for parallel magnetic field, all the domain can be modeled.

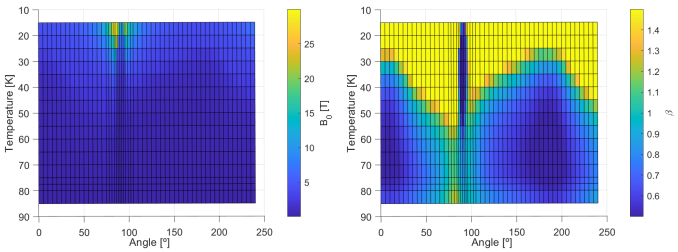

(a) B_0 **(b)** β

Figure 7: Kim Plus parameters as a function of temperature and magnetic field angle for SuperPower AP.

Plotting the Kim Plus parameters (Figure 7) make analysis of the tape's behavior go more in depth but more complicated, as there are 2 parameters in total. Unlike the original Kim model, B_0 drops to 0 when temperatures are low and the magnetic field is parallel. On the same page, β also dips to zero on the same conditions and this is because the critical current barely changes on these conditions and the algorithm tries to achieve a straight line. However, for other areas of the domain, β tends to change considerably. Upon further inspection, β can be used to identify the 2 types of peaks. As an example, for 20 K, there is a peak due to stacking fault defects that begins at 75° for low magnetic field and rapidly converges to 90°. The peaks result in flattened out critical currents which means a lower β. When there are no peaks, then the defects are not maintaining high critical currents and there is a rapid decline in these currents, resulting in higher values of β.

In conclusion, Kim Plus offers very good performance while boasting having only 2 parameters. Additionally, it allows to easily verify the location of the peaks caused by ion irradiation and stacking faults by visualizing the parameter β. However, the parameters change a lot which means that its implementation in simulator software would require an interpolation of the parameters and/or the use of a look up table in order to decide, in each iteration, which of the parameters to use based on the local operating conditions, which could lead to problems such as much higher computation times.

C. Custom Kim Model

According to Figure 8, results are good overall but, unfortunately, errors are too high for the important temperature of 77.5 K, for high parallel magnetic fields and for all perpendicular fields.

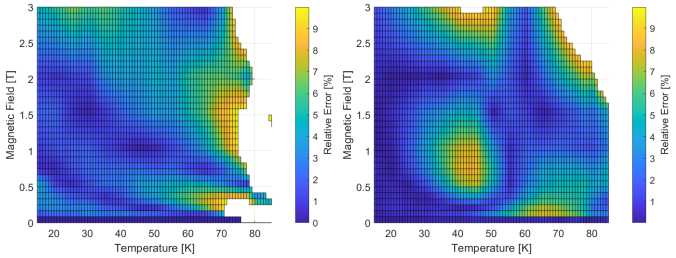

Figure 8: SuperPower AP critical current relative error ($\leq$ 10%) between database and Custom model predictions.

It is important to visualize the angle dependence of the current in order to identify the potential problems of the model (Figure 9). The first identifiable problem is that for low external magnetic fields ($B \leq 0.3$ T), the perpendicular current peaks are still not formed. However, the model recognized that they exist for higher fields and attempts to model them. This is a reoccurring phenomenon on many temperatures and is responsible for multiple inconsistencies. It is important to note that, for $B = 3$ T, the shape of the critical current sheet density seems adequate but the two curves are distant from one another. This is due to the Kim Plus part of the equation, the foundation on top of which this customized model was built upon. Therefore, if the foundation could not predict critical currents for high values of magnetic field for $T = 77.5$ K, then this model will not be able to do it too. Additionally, the stacking fault current peak starts at 86° and gradually approaches to 90°. The model decides that the best location to place the peak (in order to reduce the RMSE) is at 86°. In some occasions, the width of the database peak is short, which results in considerably high relative errors. Additionally, the width also changes heavily (namely diminishes) as the field increases which leads to even more errors, while the fitted curve has approximately the same shape. In fact, only the amplitude is changed since, in (5), the incrementing field density B is multiplied by the weight w_B.

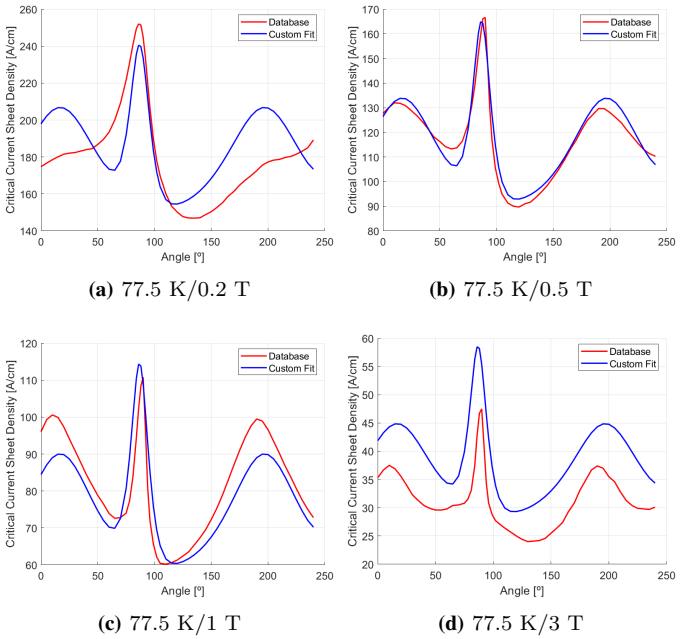

(a) 77.5 K/0.2 T **(b)** 77.5 K/0.5 T

(c) 77.5 K/1 T **(d)** 77.5 K/3 T

Figure 9: SuperPower AP critical current sheet density dependence on magnetic field angle: database and Custom model predictions. For $T = 77.5$ K, the computed parameters are $B_0 = 0.052$ T, $\beta = 0.687$, $SF_a = 0.445$, $SF_w = 8.535$, $SF_p = -2.637°$, $IR_a = 0.630$, $IR_w = 0.400$, $IR_p = 16.968°$.

Regarding the parameters introduced in customized model, they are constants that attempt to describe amplitude, location and width of each peak. It is useful to analyze their behavior as temperatures changes (Figure 10).

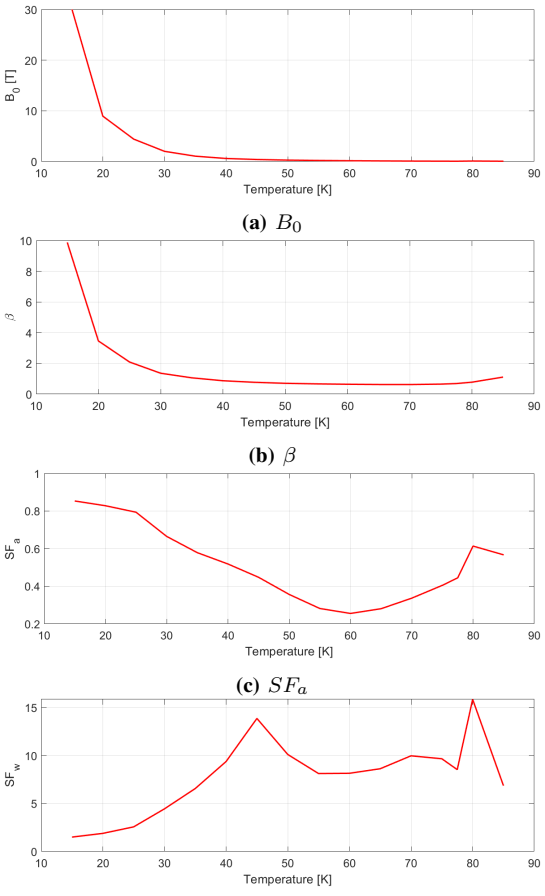

(a) B_0

(b) β

(c) SF_a

(d) SF_w

Figure 10: Custom model parameters as a function of temperature for SuperPower AP. Continues on next page.

The parameters B_0 and β behave as expected and as explained in the previous models.

Focusing now on the parallel peak, characterized by SF_a, SF_w and SF_p, it is noticeable that it tends to decrease in normalized amplitude as temperature increases, which makes sense as the tapes seem to become more sensible to magnetic field for high temperatures. Another sign of this is that SF_w tends to increase, which means the width actually decreases for higher temperatures (the peaks look more like spikes).

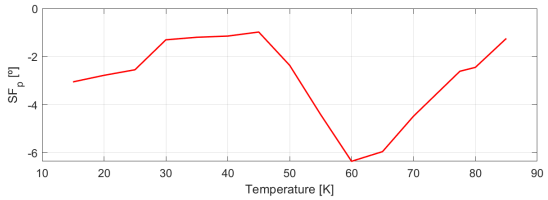

(e) SF_p

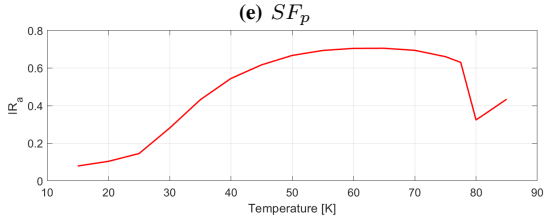

(f) IR_a

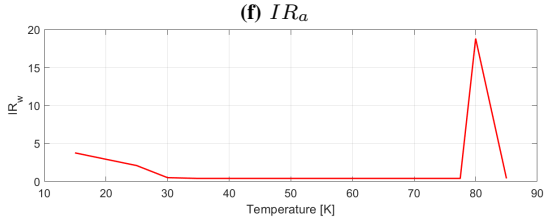

(g) IR_w

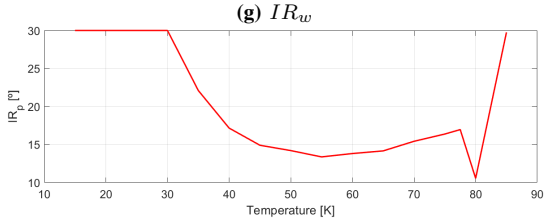

(h) IR_p

Figure 10: Custom model parameters as a function of temperature for SuperPower AP, continued.

Therefore, the angle difference between the maximum current point of the peak and half that value is lower. This can cause very large errors because the spikes are always modeled with the described normal distribution-like exponential, which is not always appropriate. There is another problem related to the location of the stacking faults peak. As mentioned before, this peak will change its center based on the applied magnetic field, and so the algorithm fits it into the angle that most reduces the RMSE. There is no clear pattern that can be seen in analyzing the SF_p parameter.

Regarding the current peak related to ion radiation, its normalized amplitude actually increases with temperature, which might suggest that the vertical defects caused by the bombardment of the ions, are only able to hold magnetic field lines in place for specific conditions. Additionally, IR_w is essentially always very low, and this is because these defects, when able to confine the fields, are able to do it for higher ranges of tape orientation. One plausible explanation for this is that the defects are not all directed the same way. In the example of 50 K for the Superpower sample, the average orientation of the defects is $15°$ but, independently of being normally distributed or not, it is evident that they come with high variance, resulting in low IR_w and consequently high peak widths. Finally, regarding IR_p, not much can be said of its behavior, outside the fact that the $30°$ values in $15-30$ K only happen because the peak amplitudes are very low (≈ 0.1) and basically are not defined, as in, they do not exist but the program converges into a local minima where raising the parameters slightly helps minimize RMSE, but it is likely that no importance should be given to these specific parameters.

The question now is if the chosen parameters should be able to change as magnetic field increases, that is, if there is not only angle dependence but also field dependence in relation with the peak's properties. Analysis of the data suggests that, for a given temperature:

1) The normalized amplitude of the ion radiation peaks IR_a changes based on the temperature and magnetic field applied. For very low temperatures (20 K) these peaks do not even appear ($IR_a = 0$) and for very high temperatures (77.5 K) the peaks start appearing for low values of external magnetic field (0.2 T). In intermediate cases (e.g. 40 K) it takes more magnetic field to cause the ion radiation peaks to appear. Therefore, depending on the operating conditions, the normalized amplitude could be approximately constant or heavily change;
2) The normalized width of the ion radiation peaks IR_w is approximately constant;
3) The location of the ion radiation peaks IR_p is approximately constant. Any deviations do not cause big relative errors because these peaks tend to be relatively wide. Additionally, they happen to be approximately constant independently of the sample having narrow bridges patterned into them (this concept will be further explained in point 6);
4) The normalized amplitude of the stacking faults peaks SF_a can be modeled as a constant;
5) The normalized width of the stacking faults peaks SF_w can vary substantially on some samples which leads to enormous relative errors;
6) The location stacking faults peaks SF_p is peculiar. For some samples it remains completely constant as magnetic field is introduced and increased. For others, it begins at around $70°$ and converges to a value closer to the expected $90°$ center (usually around $85°$). For this latter case, the model will fit the SF_p parameter to an intermediate value (e.g. $80°$) which leads to high errors. The reason for this phenomenon is related to the fact that, before measuring the critical current values in the test bench, these tapes were patterned with a narrow current bridge in order to make the measurements with a low enough current so that the test bench would not reach the current limit. It happens especially at low temperatures and fields (≤ 0.5 T). According to Dr. Nick Strickland, there are magnetic fields trapped in regions close to the bridge where the current is measured, resulting in field contributions in this area. The trapped magnetic fields are caused by the previous measurements at different angles and result in this hysteretic behavior, which implies that if the tape was rotated in the inverse direction, then the peaks would start appearing in the other side.

D. Advanced Custom Kim Model

This model has the aim of minimizing the areas of the domain where the relative error is bigger than 10%. Considering the fact that the critical current measured values are dependent on how the measurement is done, as described in point 6 of Section V-C, this model is adapted to the database studied in this work. Therefore, modeling critical current from other sources of data could benefit from modifying the present model. As an example, if there are no narrow bridges in the samples, then the parameters SF_{pi}, SF_{pf}, SF_{ps} could be converted into the original constant SF_p.

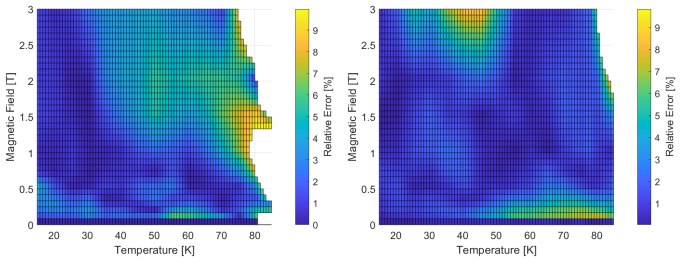

(a) 0° **(b)** 90°

Figure 11: SuperPower AP critical current relative error ($\leq 10\%$) between database and Advanced Custom model predictions.

Comparing Figures 8 and 11, showing the relative errors of the Custom Kim model and the Advanced Kim model respectively, it is clear that the latter model helped reduce the overall errors, and that is especially true for perpendicular magnetic fields and high temperatures, which are the areas where the tapes are most sensitive to the magnetic field. With the latter model, it is possible to accurately predict the critical current values for 77.5 K and 0° which is perhaps the most important operating point.

Figure 9 is now replicated in Figure 12 with this new model. The perpendicular peaks are now rapidly increasing for low magnetic field values and then stay approximately constant which seems to be in accordance to the database values. The worst example is for when the external magnetic field is 3 T, as for this case the peaks actually seem to decrease but the model does not account for this. However this seems to be a rather rare event and is happening on an extreme operating point (high temperature and field).

The problem regarding the shift in the location of the parallel peak is also mostly corrected as the model is able to follow it. It is also possible to visualize the angle of the middle peak decreasing steadily. Even though the relative errors seem much better, there are still cases when the errors accumulate:

- Errors related to magnetic field dependence - no matter how well the angle dependence is done, if the critical current decreases as magnetic field increases with a different shape than the one modeled by Kim Plus, then the errors will accumulate.
- Impulse modeling - in this work, the peaks are modeled by periodic impulses using a variation of the normal distribution. This works well in most cases but occasionally, the peaks have a more triangular shape or have a very high apex with very high surrounding derivatives. This results in the fact that very low deviations in SF_p result in high relative errors. Advanced Custom Kim was partially created to fix this issue but it seems more work is needed in this area. While calculating the relative error plots the results can seem very bad but one can visualize that graphically the curves are very close. One potential way to fix this issue is to use a completely different model for the impulse or to use a different value as the basis of the exponent i.e. using a instead of e where $a \neq e$. This a value could even be a different parameter and to be optimized during the fitting.
- IR_a modeling - although these parameters seems to behave similarly to SF_p, the fitting procedure makes it so that the peak increases when it shouldn't. Perhaps a better equation for the modeling of IR_a should be used.
- Lack of the complete angle dependence - the database is very rich in data points but only contains data ranging from 0° to 240° which means it is not possible to see the current as the tape does the full 360° rotation. It would also make it easier to study other factors like hysteresis.

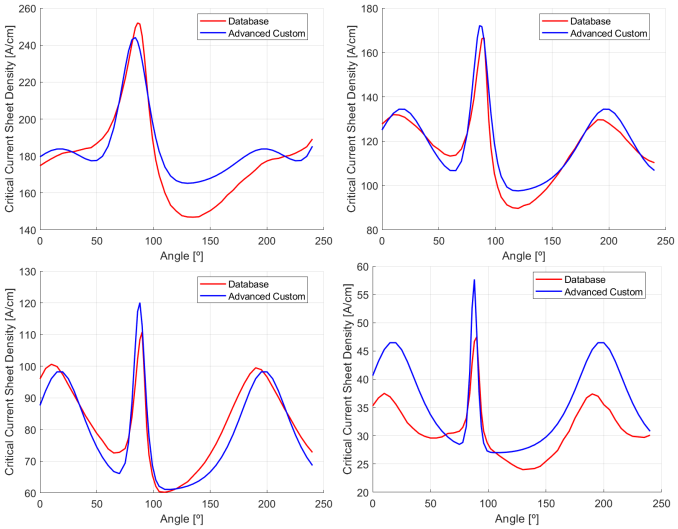

Figure 12: SuperPower AP critical current sheet density dependence on magnetic field angle: database and Advanced Custom model predictions. For $T = 77.5$ K, the computed parameters are $B_0 = 0.102$ T, $\beta = 0.791$, $SF_a = 0.574$, $IR_w = 1.001$, $IR_p = 17.480°$. The rest of the parameters are displayed in Figure 14.

Regarding Figure 13, not much is new comparing to Figure 10. All the presented parameters behave in the same way they did in the Custom Kim model. The most notable aspect is that, since there are new parameters that follow the magnetic field-dependent aspects of the peaks, slightly less importance will be given to B_0 and β and these will therefore have a smaller variance, towards the less sensitive areas of the domain (low temperatures). Addressing the remaining parameters:

- SF_a are very similar, which makes sense considering there was no change in the models regarding normalized amplitude of the parallel peak;
- Both IR_p are approximately the same and the only exception for this is when IR_a is very low which means

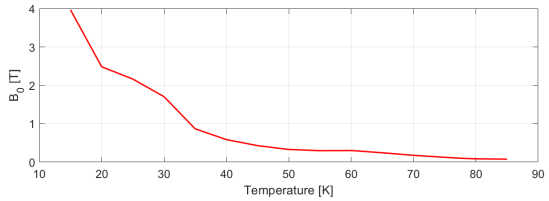

(a) B_0

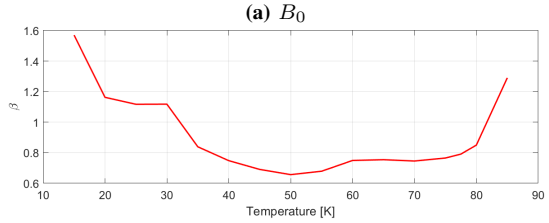

(b) β

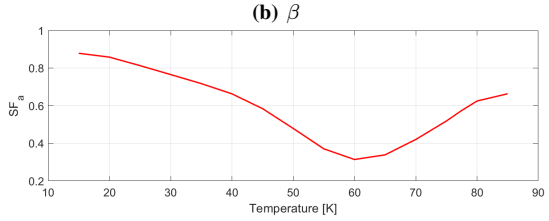

(c) SF_a

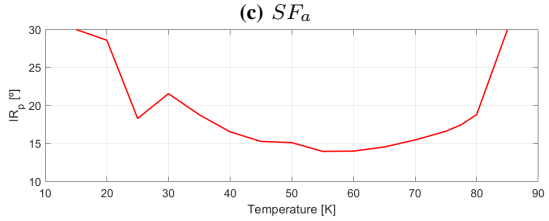

(d) IR_p

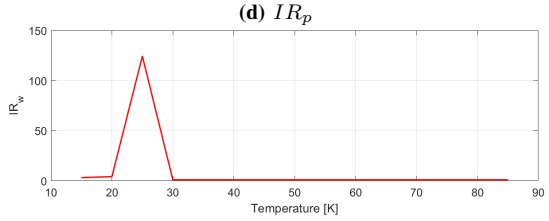

(e) IR_w

Figure 13: Advanced Custom model non-magnetic field depedent parameters as a function temperature for SuperPower AP.

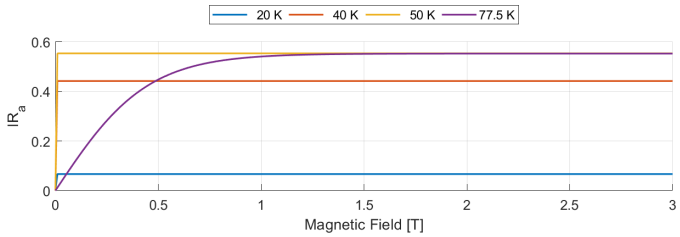

(a) $IR_a = IR_{af} \cdot \tanh(IR_{as} \cdot B)$

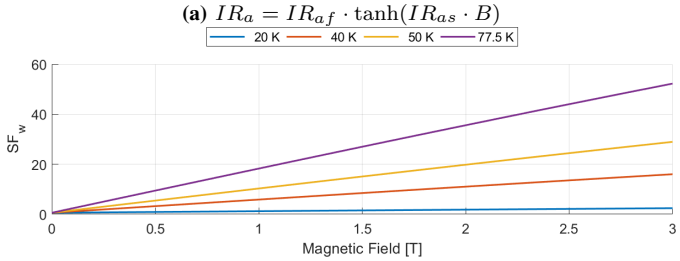

(b) $SF_w = SF_{wi} + SF_{wf} \cdot \tanh(SF_{ws} \cdot B)$

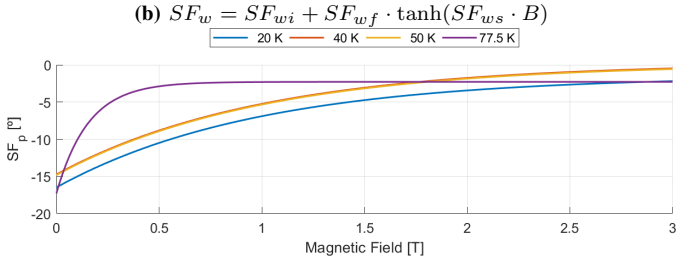

(c) $SF_p = -SF_{pi} \cdot \exp(-SF_{ps} \cdot B) + SF_{pf}$

Figure 14: Advanced Custom model magnetic field dependent parameters as a function of magnetic field for SuperPower AP.

that the normalized amplitude of the perpendicular peak is so low that the it's location and width aren't meaningful;

- IR_w is essentially very low for most of the domain for reasons explained previously.

Analyzing IR_{as}, IR_{af}, SF_{wi}, SF_{wf}, SF_{ws}, SF_{pi}, SF_{pf} and SF_{ps} turns out to be very non-intuitive compared to analyzing the previous parameters and therefore Figure 14 was created as a solution. Essentially, the equivalent IR_a, SF_w and SF_p were plotted for each temperature in accordance to (9), (10) and (11), denoted in Section III-C. Regarding these three parameters:

- IR_a - For 20 K, there is essentially no perpendicular peak which is something already discussed before. For 77.5 K, this improved model is able to follow the increase of the peak's amplitude as magnetic field increases and is fulfilling its function somewhat optimally. For 40 K and 50 K, the fitting makes it so that the value rises to its maximum for the whole span of magnetic field. Analyzing the angle dependence for these temperatures, it is possible to visualize that the peak should be appear later (usually when $B = 0.5$ T). At these instances of transition (i.e. when the perpendicular peaks emerge), the angle dependency plots can take a peculiar shape that the model is not able to imitate. However, relative errors are not enough to beach the 10% limit.
- SF_w - The first aspect to notice is that for all temperatures, the parameter increases approximately linearly with applied magnetic field. However, this does not mean that the width of the periodic exponential impulses decreases linearly. As an example, if $SF_w = 1$, then the Full Width at Half Maximum (FWHM) is measured to be about 1.2 rad, but if $SF_w = 2$ then the FWHM value becomes 0.8 rad. It is quite clear that for this sample, the width of the peaks are smaller for higher temperatures which again demonstrates the sensitivity of these tapes for high temperatures to external magnetic field.
- SF_p - As hypothesized previously, it does seem that the shifting of the parallel peak's location from the direction of rotation of the tape happens with more intensity as the temperature decreases. As an example, for 0.5 T and 77.5 K the fitted location is $90° - 3° = 87°$ and for 20 K it happens to be $90° - 11° = 79°$.

VI. Machine Learning vs Empirical Modeling

The customized empirical models have larger areas of domain where the relative error is smaller than $\leq 10\%$ when compared to the best GPR models but are significantly more complex considering there are 15 parameters in total in the case the Advanced Custom Kim Model. Additionally, this model was designed specifically for the database utilized in this laboratory and using ML is theoretically able to adapt to other databases automatically. One could use the Custom Kim Model as an alternative which has a smaller number of parameters but the performance worsens, especially on the 77.5 K temperature, which is arguably the most important one.

Another advantage of Empirical Modeling over Machine Learning is the sheer size of the created files and the computing time - a table structure containing all data from all datasets in addition to all the parameters for each of the empirical models has a size of 21 kB and requires a total of 60 minutes to compute, while a single ARD model for one HTS sample occupies 150 kB and more than 2 hours to be obtained using less than 50% of the available data as training data. Considering that GPR has a complexity of $O(n^3)$ [14], this procedure can be computationally expensive.

Neither GPR nor empirical models have been shown to be able to predict critical currents for very steep peaks, which is the main cause for areas of the domain with high relative errors. Nevertheless, the predictions on these cases are most of the times lower than the true values and that makes the models safer if used in control systems for actual applications, since the data is being lessened.

VII. Conclusion

The main objectives of this work are to apply Machine Learning (Gaussian Process Regression) and Empirical Modeling techniques to the processed public High-Temperature Superconductor database in order to verify which of the created models are appropriate for modeling the critical current of selected samples based on their operating conditions: temperature, external magnetic field magnitude and angle. On the ML front, the default and ARD variants of the software's built-in kernels are studied: Exponential, Matern variants, Squared Exponential and Rational Quadratic. Regarding the empirical models, the original Kim model is used as a starting point (in addition to Kim Plus) and are further developed in order to incorporate the angle dependence of the HTS tapes to allow more precise and easier simulations, performed in multiphysics software. This resulted in the creation of the named Custom model and Advanced Custom Model.

The best ML model was ARD Matern32, which only had significant errors when the critical current presented extremely high steepness as is the case for 45 K and 77.5 K for high fields. This model took 2 hours and 20 minutes to compute using only 50% of the data as training data.

The original Kim model tends to have low relative errors for low temperatures (≤ 50 K) but the opposite happens for high temperatures. The focus is on the 77.5 K temperature point which is the boiling temperature of nitrogen. The Kim Plus variant achieves much better results in all domains and only increments the number of parameters to be fitted by one. However, for very high temperatures (including the 77.5 K point) the results are very inconsistent and sometimes not appropriate. The Custom model increments the number of parameters up to 8 but allows for angle modeling. The downside is that the relative errors are slightly worse than Kim Plus and this makes the data very unreliable for 77.5 K. It is noted that some of these bad results are related to how the current measurements were made in the test bench which cast some light into some critical current shapes that were not expected. Lastly, the Advanced Custom model was created to provide much better relative errors (by adapting to the database) and this was achieved but at the cost of introducing even more parameters (totaling 13).

The GPR models are the simplest ones to create and, if the proper kernel is chosen (ARD Matern32), can provide very good results, but at the cost of time of computation. The Advanced Custom Model is the one with the greatest area of domain with low relative errors (including 77.5 K) and boasts low computing times when compared to GPR, but requires much more fitting complexity and a grand total of 13 parameters to be fully described.

References

[1] Z. Melhem, *High temperature superconductors (HTS) for energy applications*. Woodhead Publishing, 10 2011.

[2] T. P. Sheahen, *Introduction to High-Temperature Superconductivity*. Springer US, 2002.

[3] "Robinson Research Institute - Victoria University of Wellington." [Online]. Available: https://www.wgtn.ac.nz/robinson

[4] N. Strickland, C. Hoffmann, and S. Wimbush, "A 1 kA-class cryogen-free critical current characterization system for superconducting coated conductors," *The Review of scientific instruments*, vol. 85, p. 113907, 11 2014.

[5] "Robinson HTS wire critical current database." [Online]. Available: http://htsdb.wimbush.eu/

[6] S. C. Wimbush and N. M. Strickland, "A public database of high-temperature superconductor critical current data," *IEEE Transactions on Applied Superconductivity*, vol. 27, pp. 1–5, 2017.

[7] Y. B. Kim, C. F. Hempstead, and A. R. Strnad, "Magnetization and critical supercurrents," *Physical Review*, vol. 129, p. 528, 1 1963. [Online]. Available: https://journals.aps.org/pr/abstract/10.1103/PhysRev.129.528

[8] W. Woch, R. Zalecki, A. Kołodziejczyk, O. Heiml, H. Sudra, and G. Gritzner, "Kim-type critical state models and critical currents of thallium based superconductors," *Acta Physica Polonica A*, vol. 114, pp. 99–106, 7 2008. [Online]. Available: http://przyrbwn.icm.edu.pl/APP/PDF/114/a114z113.pdf

[9] "Gaussian process regression - MATLAB and Simulink." [Online]. Available: https://www.mathworks.com/help/stats/gaussian-process-regression.html?s_tid=CRUX_lftnav

[10] "Fit a gaussian process regression (GPR) model - MATLAB fitrgp." [Online]. Available: https://www.mathworks.com/help/stats/fitrgp.html

[11] D. Singh and B. Singh, "Investigating the impact of data normalization on classification performance," *Applied Soft Computing*, vol. 97, p. 105524, 12 2020.

[12] C. E. Rasmussen and C. K. I. Williams, *Gaussian Processes for Machine Learning*. The MIT Press, 11 2005. [Online]. Available: https://direct.mit.edu/books/book/2320/Gaussian-Processes-for-Machine-Learning

[13] K. Liu, Y. Li, X. Hu, M. Lucu, and W. D. Widanage, "Gaussian process regression with automatic relevance determination kernel for calendar aging prediction of lithium-ion batteries," *IEEE Transactions on Industrial Informatics*, vol. 16, pp. 3767–3777, 6 2020.

[14] J. Wang, "An intuitive tutorial to gaussian processes regression," 2020. [Online]. Available: https://arxiv.org/abs/2009.10862